Tube Skin Temperature Prediction of Catalytic Reforming Unit (CRU) Heaters

*SUZANA YUSUP , NGUYEN DUY VINH, NURHAYATI MELLON & ABDULLAH HASSAN**
*Chemical Engineering Programme
Universiti Teknologi PETRONAS, Bandar Seri Iskandar 31750, Tronoh,Perak.
MALAYSIA.
**PETRONAS Penapisan (Melaka) Sdn. Bhd,.PP(M)SB, Malaysia.

Abstract: The maximum duty of reformer heaters is governed by the occurance of maximum tube skin temperature of the heaters. The value of maximum tube skin temperatures of the heaters must not exceed theirs' maximum allowable design temperature. The paper highlights the simulation of the tube skin temperatures of CRU heaters and temperature distribution across the heater tubes. The simulated results are important in order to access the heaters performance and prediction of the coke formation in tubes. The simulated results are verified using Plant data. The simulation is done using finite element approach. A two dimensional model is developed with a front view and a cross-sectional view for each heater. The maximum percentage deviation of predicted tube skin temperature using Finite element approach was found to be 1.2 % .

Key-Words: Simulations, Tube furnance, Finite Element, coke formation.

1 Introduction

In a heater, tube skin temperature is one of the most important parameters that need to be closely monitored since it dictates the overall performance of the heater. Moreover, it can also be an indicator of coke formation in the heater's tubes. A high tube skin temperature is a result of refinery fired heater heat-flux imbalances that can cause high coke-formation rates. The materials of the heater's tubes can only withstand a maximum allowable tube skin temperature. When this temperate is reached, either heater firing must be reduced or the heater must be shut down for coke removal. Thus, the developed model can give an indication of the heaters' performances and shutdown periods for coke removal.

For the past four decades, catalytic reforming of naphtha has evolved rapidly to become one of the most advanced processes in the refining industry. The main objective of the process is to convert low-octane naphtha to high-octane reformate to be used as high performance gasoline fuel. Alternatively, the naphtha reformer unit can also produce high yields of aromatics for petrochemical feed-stocks. Today, reforming technology, catalysts and processes continue to lead petroleum refining in innovation, safety, and reliability as well as environmental impact and profitability. Moreover, because of some environmental regulations on gasoline burning wastes, refiners and catalyst manufacturers are trying to find means for catalyst performance improvement and process design improvement to enhance the selectivity to aromatics and high-octane reformate. All these researches and studies aim at the following objectives:

- Higher reformate octane yields
- More efficient catalyst regeneration
- Longer catalyst life and enhanced surface stability
- Lower-pressure operation and less hydrogen recycle [1]

In industrial practice, the operating conditions of the reforming unit are usually described in terms of severity. The most widely used measure of reforming severity is the research octane number (RON). After years of operations, the catalyst deactivates; to compensate for the lower activity, the severity (reactor temperatures) of the process must be

increased. This leads to the high firing rate of the heaters of reformer unit. In this way, the required RON can be maintained at the desired level. However, this high-severity operation is at the expense of short run-length of heaters due to high firing rate, resulting in higher coke formation rate in tubes and high tube skin temperatures. At PETRONAS Penapisan (Melaka) Sdn. Bhd,.PP(M)SB, the Catalytic Reformer Unit (CRU) has been operating at 110% capacity. This situation indicates a high severity of operation. This high throughput results in high recycle gas, higher firing rate of heater, more catalyst required in the rectors and an increased load on the columns. This severity has long been put under studies and one of the equipment under close monitoring are the heaters. Because of the high firing rate, the tube skin temperatures are closing to its limits [2].

Tube metal temperatures are often monitored with skin thermocouples. Their accuracy is greatly debated; nevertheless, skin couple readings are often used to determine heater end-of-run. Once the tube metal temperature of the heater tube is reached, heater firing must be reduced or the heater must be shut down to remove coke. In the extreme case, long-term operation at high heater tube wall temperature can cause the tube to rupture [4]. Moreover, skin thermocouples are known to be vulnerable and often inaccurate, giving readings some 20 to 50°C higher than the real tube skin temperature. The higher reading is caused by the fact that the skin thermocouple construction itself may act as a heat barrier, giving the thermocouple a higher temperature than the tube wall. Skin thermocouples in reformer heaters also tend to fail quite often due to the very high tube temperatures compared to those in other process heaters.

Y. Suyadal (2006) [3], carried out experimental work on estimation of kinetic parameters for combustion process in a bench scale fluidized bed. For the modeling work they concluded that the surface reaction constant can be incoperated into a fluidized bed combustor model. Thus experimental results obtained from fluidized bed can establish the basis for the design of fluidized bed combustors. G.D Stefanidis et.al (2006), [5] simulated a steam cracking furnances using computational fluid dynamic approach. They found that a smaller flame volume has important effects on the predicted temperature distribution in the furnance as well as on other significant design design parameters like the refractory wall and tube skin temperatures.

In the present work, the simulation of tube skin temperatures of CRU heaters is carried out using FEMLAB. The Plant Information data is used to verify the model.

2 Theory

The mathematical equation for heat transfer by conduction is as shown in equation (1)

$$\rho C \frac{\partial T}{\partial t} - \nabla(k\nabla T) = Q \quad (1)$$

For steady state, equation (2) applies.

$$\nabla(k\nabla T) = Q \quad (2)$$

To model heat conduction and convection through a fluid, the heat equation includes a convection term. In FEMLAB, this formulation is represented in the Conduction and Convection application mode as in equation 3.

$$\rho C \frac{\partial T}{\partial t} + \nabla(-k\nabla T + \rho C_p T u) = Q \quad (3)$$

The heat flux vector is defined by the expression within the brackets in equation (3), which for transport through conduction and convection yields equation (4)

$$q = -k\nabla T + \rho C_p T u \quad (4)$$

Assumptions

Following are the assumptions made to simplify the modeling:

- Only one side of tube wall exposed to direct firing is modeled since the tube is symmetrical and assuming the rate of

firing is equally distributed to both sides .

- Only finite length of the tube is considered as the actual length of the tube is higher than the thickness of the tubes.
- Momentum and mass transfer are neglected.
- Constant thermal conductivity

3 Methodology

Fig.1 and Fig.2 show the flow chart followed in simulating the heater tube temperature using FEMLAB and 3-D view of the heater tube respectively.

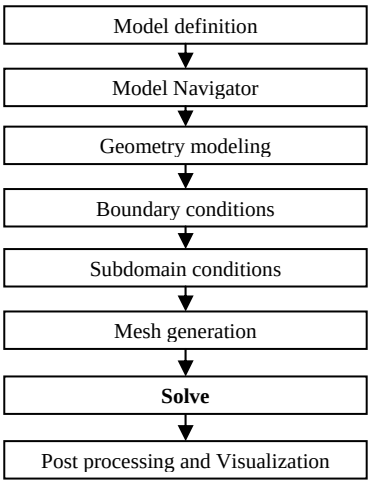

Fig.1: Flowchart in GUI of FEMLAB

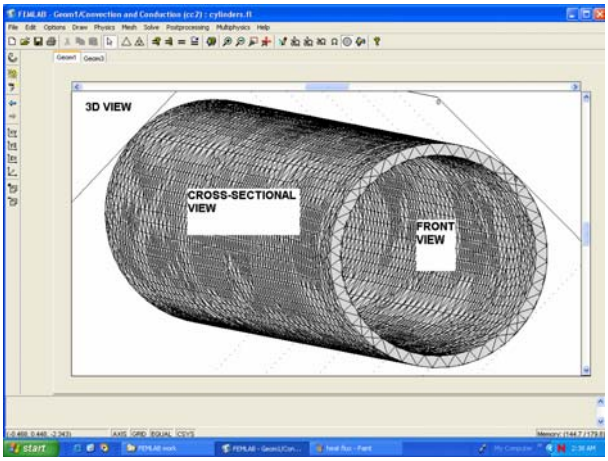

Fig.2 : 3-D view of the heater tube.

The following paragraphs highlights the overall methodology adopted as indicated in Fig.1 along with user input values. In solving the partial differential equations, *finite element method (FEM* is used). The software Version 3.0 runs the finite element analysis together with adaptive meshing and error control using a numerical solver.

Fig.3 – Fig.9 show the window under each steps of the simulation.

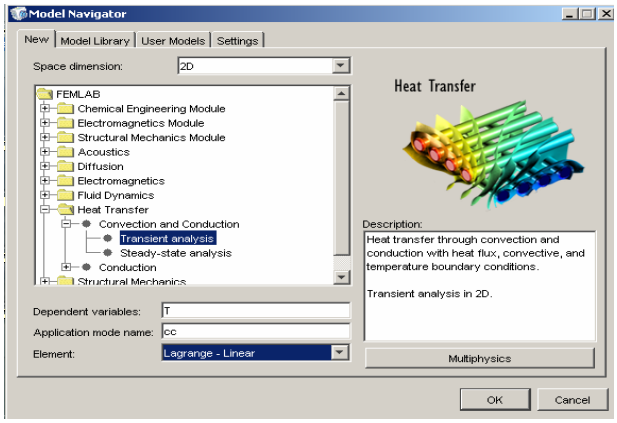

Fig. 3 Model definition window

The characteristics of tube front view (2D) as in Fig.2 are as follow:

- Conduction and Convection heat transfer – Transient analysis
- Shape - Circle
- Domain:
  - Outside diameter: 0.1143 m
  - Inside diameter: 0.1023 m
- Boundary conditions:
  -Heat flux Q
  -Process side temperature $T_{process}$

The characteristics of cross-sectional view of the tube in 2D as shown in Fig.2 are as follow:

- Conduction and Convection heat transfer – Transient analysis
- Shape – Rectangle (due to the assumption of equal heat flux on both sides and symmetry of the tubes)
- Domain: 0.00602 m $\times$ 0.0.5 m
- Boundary conditions:
  -Heat flux Q
  -Process side temperature $T_{process.}$
  -Inlet temperature
  -Outlet temperature

Model navigator

In model navigator window as in Fig.4, the following criteria are selected.

Model: Convection and Conduction heat transfer – Transient analysis (as shown in Fig.4).

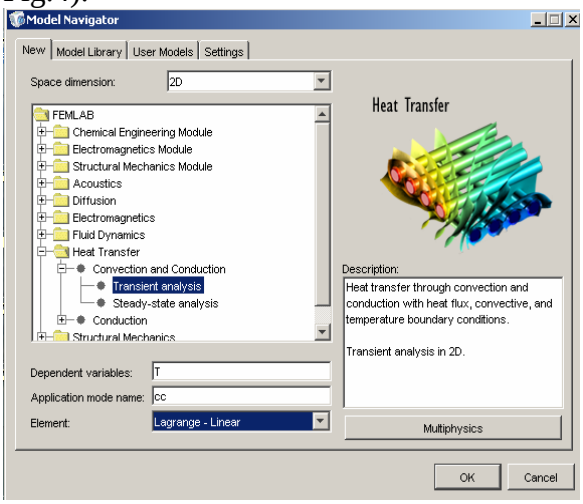

Fig.4: Model navigator window

Geometry modeling

Fig.5 shows the dimension of the tube.

- The front view – Circle
  - Outside diameter: 0.1143 m
  - Inside diameter: 0.1023 m
- The cross-sectional view – Rectangle (0.00602 m ×0.0.5 m)

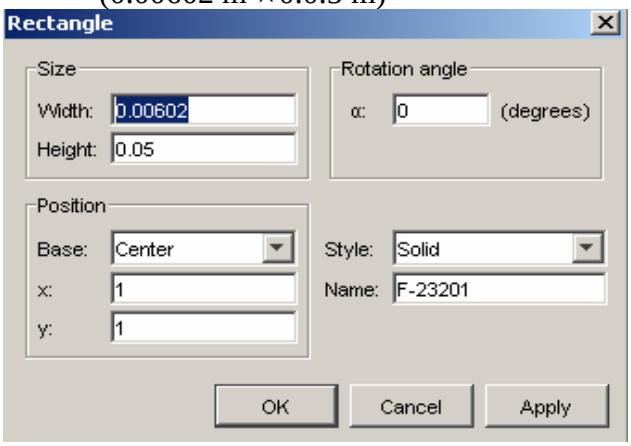

Fig.5: Geometry modeling window

Boundary condition

Fig.6 shows sample window for boundry condition setting.

The front view

-Heat flux Q

-Process side temperature $T_{process}$

The cross-sectional view

-Heat flux Q

-Process side temperature $T_{process}$.

-Inlet temperature

-Outlet temperature

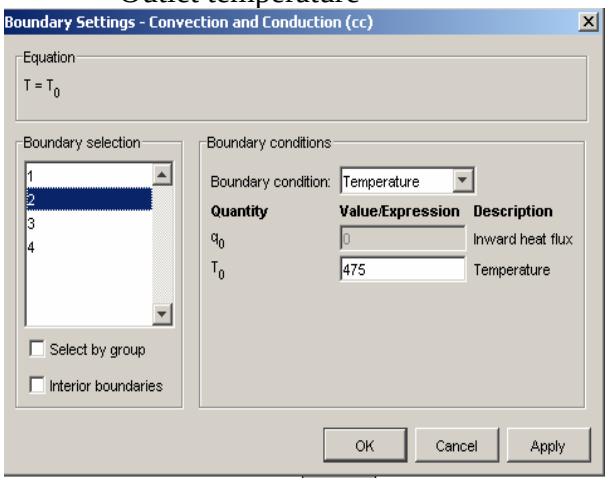

Fig.6: Boundry condition window

Subdomain

The subdomain settings include: thermal conductivity, density, heat capacity, heat source and initial temperature (as shown in Fig.7).

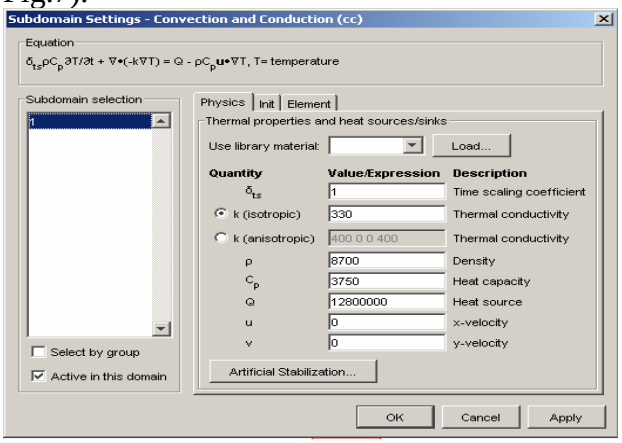

Fig.7: Subdomain window

Mesh generation and Solve

After all the conditions have been set for boundaries and subdomains, the mesh is generated to determine the degrees of freedom to be solved for the PDEs followed by Solve command. These steps are shown in Fig.8.

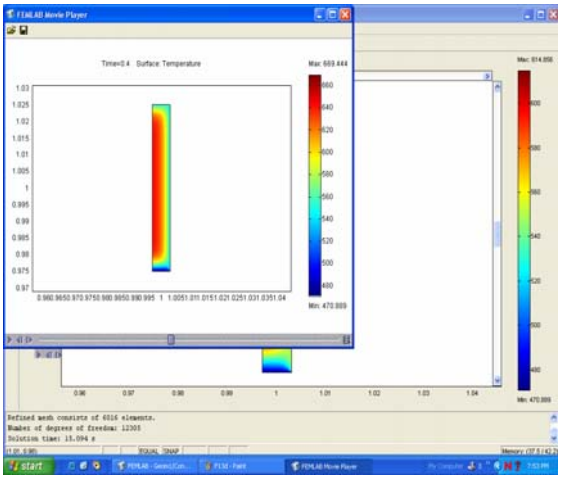

Fig.8: Mesh generation window

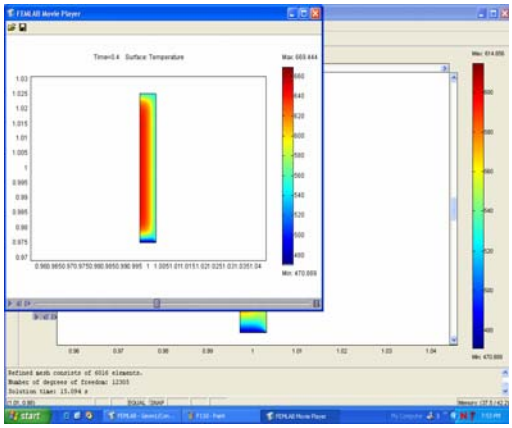

Fig.9: Post processing window

Post processing and Visualization

Once a solution is satisfied, the solution is post-processed. Post processing steps include 3D, animation, contour plot, boundary plot and heat flux plot. Fig.9 shows the animation features of the post -processing mode. In this mode users can view the change of temperature profile with respect to time.

4 Result and Discussion

The simulation results of tube skin temperatures of the four CRU heaters are shown in Fig.10. The temperature distributions for all four heaters exhibit the same trend, as shown in Fig 10 and Fig.11. The tubes wall temperature that was exposed to firing has the highest temperature. The values of the tube skin temperatures for all four heaters are summarized in the following Table1. For all the cases, the temperatures were found to decrease across the tube to the fluid side.

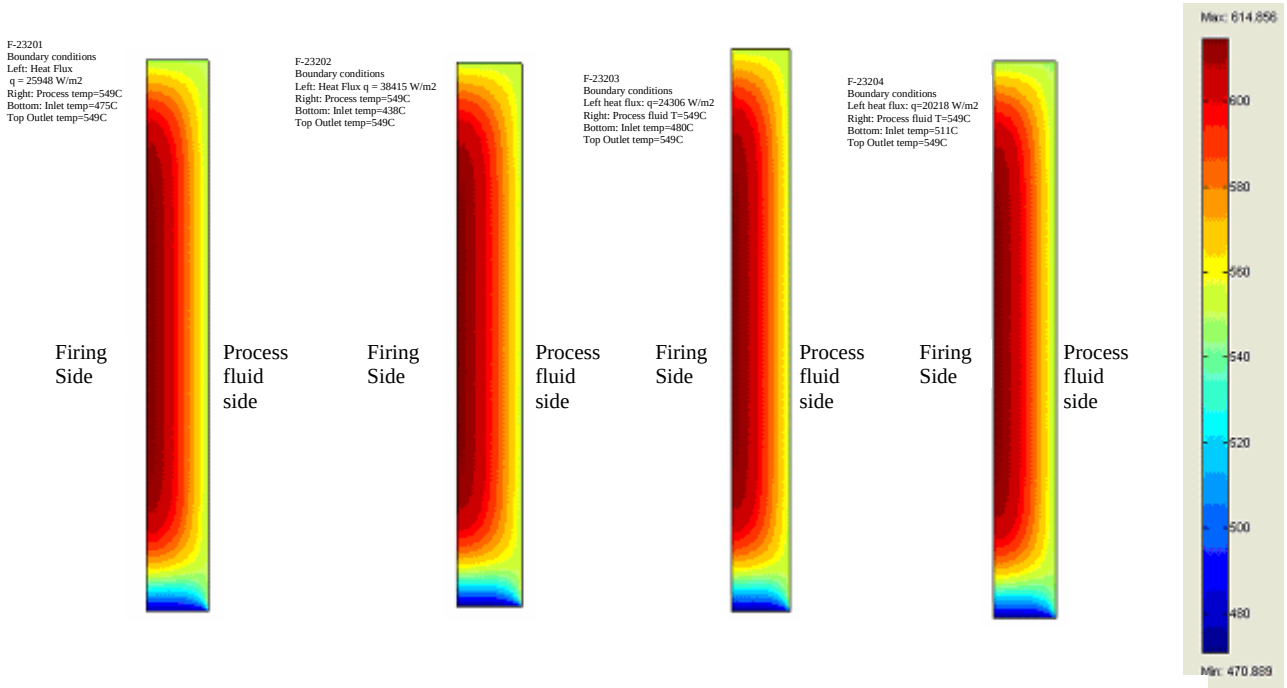

Fig. 10: The horizontal cross-sectional view for tube skin temperarature of Heater1: F-23201, Heater2: F -23202, Heater3: F23203, Heater4: F23204

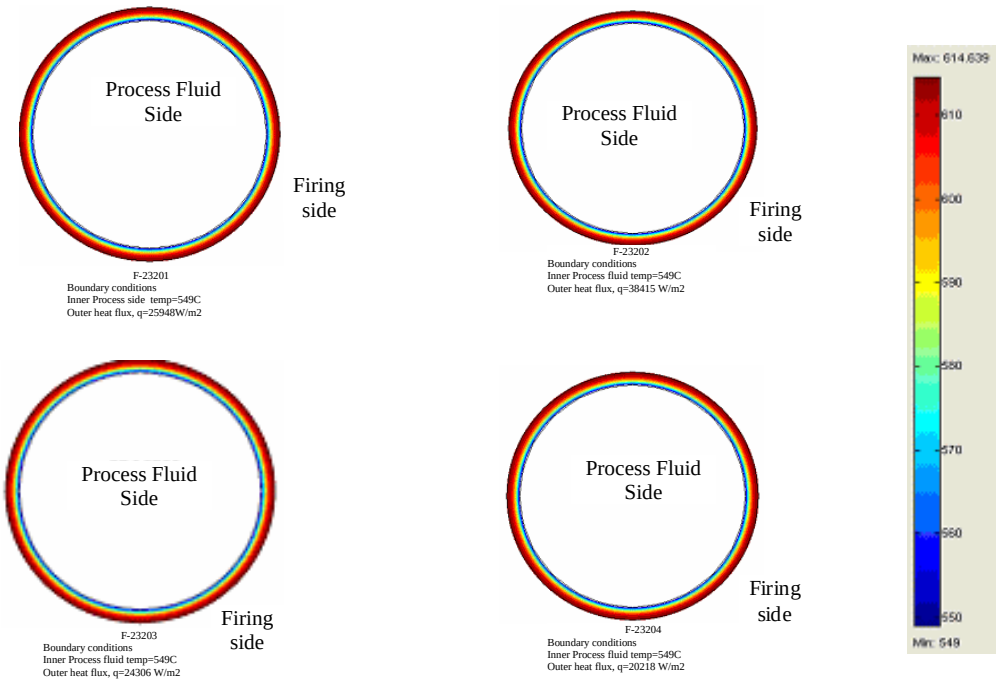

Fig. 11: The front view for tube skin temperarature of Heater1: F-23201, Heater2: F -23202, Heater3: F23203, Heater4: F23204

Table 1 shows the comparison between the tube skin temperatures of actual heaters obtained after turnaround with that predicted through FEMLAB simulation. For all the four heaters, simulation results give slightly higher values of the tube skin temperature.

Table1 Tube skin temperature of Heaters

HEATER 1: f-23201		
Operating parameters	Base case (15/02/2005)	FEMLAB design case
$T_{skinmax}$ (^oC)	**612.04**	**614**
HEATER 2: f-23202		
Operating parameters	Base case (30/04/2005)	FEMLAB design case
$T_{skinmax}$ (^oC)	**593.78**	**601**
HEATER 3: f-23203		
Operating parameters	Base case (09/02/2005)	FEMLAB design case
$T_{skinmax}$ (^oC)	**597.28**	**600**
HEATER 4: f-23204		
Operating parameters	Base case (09/04/2005)	FEMLAB design case
$T_{skinmax}$ (^oC)	**578.15**	**582**

The difference in the maximum tube skin temperature between the two cases is 7.22^{o}C with % difference of 1.2%, for F-23202 heater. The other heaters exhibit smaller differences approximately, 2 to 4^{o}C. Thus, based on the results shown in Table 1, a recommendation can be made as to further increase the firing rate since the maximum allowable tube skin temperature of 650 ^{o}C is not reached. By increasing the firing rate in a controllable manner, the required research octane number (RON) can be maintained at the desired level and coke formation within the tube can be avoided.

Variations of operating variables

The change in the tube skin temperature values, under influence of variation of heat flux, heater tubes inlet and outlet temperatures are also studied. As the heat flux is increased by 10% of its current value to 28542 W/m^2, the tube skin temperature was found to increase from 614 ^{o}C to 620 ^{o}C as shown in Fig 12.

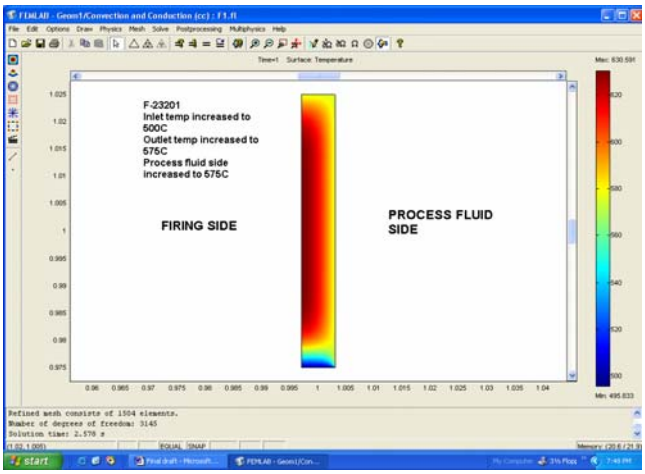

Fig 12: Effect of varying heat flux of Heater1.

When the inlet temperature of F-23201 tube increases to 500 ^{o}C and the process fluid side temperatures increase to 575 ^{o}C, the tube skin temperature was found to increase from 614 ^{o}C to 630 ^{o}C. Thus, the developed model, can be used to predict the trend of the tube skin temperature of the heater when subjected to variation of operating condition such as variation of the heat flux, and the inlet and outlet temperature of the process fluids.

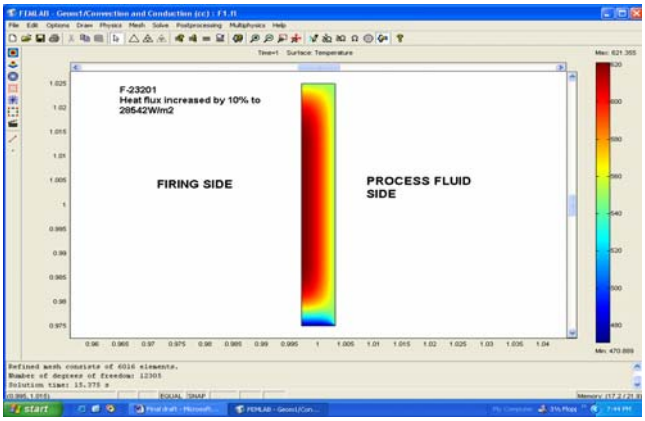

Fig 13: Effects of varying inlet and process fluid temperatures of Heater1.

5 Conclusion

It is deduced that the tube skin temperature depends on the heat flux and the inlet and outlet process fluid side temperatures. In addition the developed model and simulation can be used as a monitoring tool to predict the trend of tube skin temperature within the metal tube of a CRU heaters for PP(M)SB. The higher the temperature differences between the base case and design case, acts as indicator of amount of coke deposition in the actual tubes. With the simulation ability to predict the values of the maximum temperature that the heater tube can withstand, metal fatique and fracture can be avoided. The simulation can further be extended to incorporate the effect of coke deposition and variation of temperature profiles within the catalytic reformer unit in future.

Acknowledgement

The author would like to acknowledge Universiti Teknologi PETRONAS for providing the computing facilities that enable the work to be carried out.

References:

[1] Gary R. Martin, 'Heat-flux imbalances in fired heaters cause operating problems', *Hydrocarbon Processing*, 1998, pp. 1-7.

[2] Nguyen Duy Vinh, *'Industrial Internship Final Report'* June 2005.

[3] Y.Suyadal, 'Gas temperature profiles at different flow rates and heating rates suffice to estimate kinetic parameters for fluidized bed combustion', Experimental Thermal and Fluid Science, 2006,

[4] George J. Antos, Abdullah M. Aitani, Jose M. Parera,, 'Catalytic Naphtha Reforming', *Science and Technology*, Marcel Dekker, Inc. 1995, pp. 231-236.

[5] G.D.Stefanidis,B.Merci,G.J.,Heynderickx, G.B. Marin, CFD simulations of steam cracking furnances using detailed combustion mechanisms., *Computers and Chemical Engineering*, 30, 2006, pp. 635-649.

Nomenclature:

Q_{proc}	Process side heater duty, [kW]
T_{out}	Process outlet temperature of heater, [^{o}C]
T_{in}	Process inlet temperature of heater, [^{o}C]
q_{av}	Average heat flux to heater tubes, [W/ m^2]
D_o	Outside tube diameter, [m]
D_i	Inside tube diameter, [m]
lamda	Thermal conductivity tube metal, [W/ m.K]
$T_{bulkmax}$	Bulk temperature at the location of the maximum tube skin temperature, [^{o}C]
$T_{skinmax}$	Maximum tube skin temperature in the heater, [^{o}C]
u	Velocity field [ms^{-1}]